BIOCYBERNETICS AND BIOMEDICAL ENGINEERING 42 (2022) 596–614

Available at www.sciencedirect.com

ScienceDirect

journal homepage: www.elsevier.com/locate/bbe

Original Research Article

EMG-controlled hand exoskeleton for assisted bilateral rehabilitation

Berith Atemoztli De la Cruz-Sánchez [a,c,*], *Manuel Arias-Montiel* [b], *Esther Lugo-González* [b]

[a] *Control and Robotics Laboratory, École de Technologie Supérieure, 1100 Notre-Dame St W, Montreal, Quebec H3C 1K3, Canada*

[b] *Institute of Electronics and Mechatronics, Universidad Tecnológica de la Mixteca, Carretera a Acatlima km. 2.5, Huajuapan de León, Oaxaca 69000, Mexico*

[c] *Postgraduate Division, Universidad Tecnológica de la Mixteca, Carretera a Acatlima km. 2.5, Huajuapan de León, Oaxaca 69000, Mexico*

ARTICLE INFO

Article history:
Received 2 May 2021
Received in revised form
17 March 2022
Accepted 11 April 2022
Available online 11 May 2022

Keywords:
Assistive rehabilitation
EMG signals
Fuzzy control
Hand exoskeleton

ABSTRACT

This article presents an electromyography (EMG) controlled hand exoskeleton for basic movements in assisted bilateral therapy, where bimanual work is required by the user. The target users are individuals with the right hand affected by an accident or cerebrovascular problems which require passive or assisted rehabilitation. Through a Matlab GUI, the system receives, processes and classifies electromyographic signals from the user acquired by a MYO armband obtaining an accuracy of 81.2% using k-Nearest Neighbors (kNN) as the classification algorithm and Random Subset Feature Selection (RSFS) as the feature selection algorithm. Subsequently, the exoskeleton reproduces the movement detected in the user's opposite hand. The exoskeleton prototype is 8 degrees of freedom (DOF), built using 3D printing and has independent movement of the fingers. The movement controller is based on fuzzy logic. For the system performance analysis, kinematic information from a motion capture system is used to compare the trajectories in different grasping tasks of a user's hand with and without the exoskeleton with a maximum error of 10.63% and a minimum of 3.46% with the desired final position, which physically represents a difference of 1.89° and 0.07° respectively.

© 2022 Nalecz Institute of Biocybernetics and Biomedical Engineering of the Polish Academy of Sciences. Published by Elsevier B.V. All rights reserved.

1. Introduction

The acquisition and processing of bioelectric signals produced by the human body is a common topic in clinical studies to evaluate the health status of a patient. The electrical activity of cells and tissues from different organs can be recorded, such as electrocardiographic (ECG), electroencephalographic (EEG), electromyographic (EMG), and electro-

* Corresponding author at: Control and Robotics Laboratory, École de Technologie Supérieure, 1100 Notre-Dame St W, Montreal, Quebec H3C 1K3, Canada.

E-mail addresses: berithcruzs@gmail.com (B.A. De la Cruz-Sánchez), mam@mixteco.utm.mx (M. Arias-Montiel), elugog@mixteco.utm.mx (E. Lugo-González).

https://doi.org/10.1016/j.bbe.2022.04.001

0168-8227/© 2022 Nalecz Institute of Biocybernetics and Biomedical Engineering of the Polish Academy of Sciences. Published by Elsevier B.V. All rights reserved.

oculographic (EOG), which measure electrical activity in the heart, brain, muscles, and eyes respectively. The integration of biosignals to improve human-robot interaction has increased in recent years, especially in the area of medicine [1–4]. This approach improves devices that can help prevent disease [5], reduce recovery times [6] and assist healthcare personnel during medical procedures [7]. The brain-controlled hand exoskeleton reported by Li et al.[8] is an example of a robotic device controlled by biosignals. The authors proposed using the attention value as an input command for controlling the hand exoskeleton. The target users are stroke survivors during the flaccid paralysis period who need continuous passive motion training of their hands. Active rehabilitation training is carried out using an attention value threshold which is measured using an electroencephalography (EEG) sensor as a brain-controlled switch for the hand exoskeleton. Another emerging trend in biomedical science is the use of surface EMG signals (sEMG) which are non-invasive and painless to obtain, easy to implement, and whose existing systems in the marketplace are versatile [9–11]. Altin and Orhan [12] proposed the development of joysticks using sEMG signals for drone flight control. Furthermore, Ali et al. [13] developed an EMG-based interface for the control of a humanoid NAO robot for future use in the service robotics industry. The video game industry is no exception in trying to take advantage of this type of technology, with Shih-Chieh et al. [14] exploring the possibilities of implementing EMG signals to detect the movements of the players' mouths, allowing new ways of control by the user. In the literature, there are different contributions regarding the use of sEMG with robotic prostheses [15,16], devices for rehabilitation assistance [17], and for devices that strengthen the user's abilities [18]. EMG signals help to track the user's performance by obtaining electrical muscle information which provides information relating to the strength, motion range, and the physical condition of the user. In rehabilitation devices it allows the therapist to observe the progress of rehabilitation based on the fatigue information of the muscles [19].

Due to its constant use in daily life, the hand is prone to diseases and accidents that motivate researchers to propose novel and functional solutions to recover mobility, to create prostheses as well as inventing assistive devices for daily life [20]. In this context Akgun et al. [21] developed an adaptive robotic system with a simple mechanical structure to be used for hand rehabilitation. The middle and the proximal phalanxes are used as a link of consecutively connected two 4-bar mechanisms, respectively. The exoskeleton joints are actuated by a single electromechanical cylinder in order to produce flexion and extension movements. Kinematic analysis was carried out in order to design an ergonomic system suitable for the limitations of the standard range of motion. The exoskeleton was developed for only one finger and the control was implemented without the use of bioelectric signals. Since the development of algorithms in the Artificial Intelligence (AI) area, now it is possible to build more complex prosthetics and orthotics that replicate the movements of a healthy hand in a more natural way. The problem of pattern identification with AI has been formulated from different mathematical approaches and it has been used for movement intention identification of different extremities, even when they are amputated [22]. Technological advances have helped to propose complex algorithms because nowadays there are more computing capacities and hardware platforms available [16]. Some of the most common algorithms used in hand gesture recognition are Support Vector Machines (SMV) [23–25], Artificial Neural Networks (ANN) [26,27], Wavelet Deep Belief Networks (WDBN) [28], k-Nearest Neighbors (kNN) [29–32], Neuro-Fuzzy Interference Systems (ANFIS) [33] and Random Forest (RF) [34]. In sEMG signals the electrical impulses produced by the muscles during the contraction and relaxation process are associated with hand movement [31], allowing the creation of myoelectric controllers or the detection of user intent.

The device developed by Leonardis et al. [35] is an exoskeleton for bilateral rehabilitation for people who have suffered a stroke. EMG signals are used to estimate the grasping force exerted by the healthy hand on a sensorized object and transfer the same force to the paretic hand through the exoskeleton. Authors report that this approach allows the user to perform rehabilitation exercises with any arbitrary object. Similarly, the work presented in [36] detects the patient's intention with EMG signals using 3 electrodes. This work proposes a game-based rehabilitation system with kinematic feedback from a Kinect sensor and electromyographic information. Through relying on technology that provides kinematic feedback it is possible to analyze and evaluate the behavior of the exoskeleton during different tests. The works as reported in [37,38] demonstrated the advantage of combining motion capture systems with EMG signals to obtain ranges of motion and evaluate the performance of hand and knee exoskeletons. Despite the promising results reported by Arteaga et al. [37] in the classification of EMG signals (97% accurate) using a fine-KNN algorithm, authors found a strong dependence of these results on the electrodes location which could be a disadvantage due to the difficulty of placing them in the exact same position in all the tests. One of the main challenges of detecting the patient's intention through electromyography is the uncertainty in the position of the device that acquires the EMG signals, thereby affecting the classification results. However, it is possible to reduce the effect of this error with the creation of diverse EMG databases and the application of algorithms for feature selection. Hazam et al. [39] report the advantage of implementing feature selection algorithms on upper limb EMG signals based on the frequency domain.

Another issue associated with the acquisition of EMG signals is the equipment normally used, since it is heavy and sophisticated, which prevents the creation of portable systems aimed at non-expert users. There are currently different EMG signal acquisition devices commercially available that are wireless and lightweight, making them suitable for portable systems. Recently, Chen et al. [40] developed a soft exoskeleton glove for hand bilateral training which is able to carry out four types of hand motion. They use the OpenBCI GUI for sEMG signal acquisition and neural networks for the classification of the hand movements. Authors reported a mean accuracy of 98.7% for the classifier in tests with only four subjects. However, details regarding the number of subjects or the database used for the training and testing of the classifier were not provided. The main disadvantages of this

device are the complex procedures for design, manufacture and characterization of pneumatic actuators. Cote-Allard et al. [41] presented the first in-depth analysis of features learned using deep learning for EMG-based hand gesture recognition. They used a previously generated database recorded with the 3DC Armband featuring 22 able-bodied participants performing ten hand/wrist gestures. An accuracy of 81.38% was reported and it was mentioned that the main limitation of their study was the use of a single architecture to generate the learned features. The work developed by Burns et al. [42] uses Delsys EMG sensors with wireless transmission for the recognition of 15 different grips, which the HEXOES exoskeleton placed on the opposite hand must reproduce. Using information from only five participants and with an ANN algorithm, an accuracy of 67.8% was obtained. Castiblanco et al. [19] proposed an assist-as-needed exoskeleton for hand rehabilitation based on a mechanical design previously reported in the literature. It was argued that a more effective rehabilitation robotic system can be obtained by considering both the hardware and training paradigm during the design process. A Myo device sensor was used to acquire EMG signals from the user and kNN classifiers with features in the time and frequency domains. The classifiers recorded an average accuracy of 91% in tests with four patients undertaking four hand therapy movements. The exoskeleton was developed for only four fingers and the authors highlighted the complexity with the thumb's motion as a challenge when designing the hand exoskeleton. In contrast, albeit with fewer tests and for 6 grips, Zhang et al. [43] reported 92.7% accuracy using MYO, a wireless EMG signal acquisition armband. The number of tests and test subjects has an impact on the final performance of the classification algorithm. Small or single-person databases can create seemingly robust systems that fail when entering a new user's information.

Recently, diverse studies have been carried out to investigate the efficacy of the bilateral approach for improving the upper limb rehabilitation. Li et al. [44] examined the effects of two hybrid therapies, robotic priming combined with Mirror Therapy (MT) and robotic priming combined with Bilateral Upper Limb Training (BULT) in stroke survivors. The study's results indicate that both approaches showed significant benefits in the recovery of most sensorimotor functions. Hsu et al. [45] compared the impact of robotic-assisted therapy with bilateral practice (RTBP) and usual task-specific training facilitated by therapists on task and motor performance for stroke survivors from an occupational therapy point of view. The results of this study suggest that RTBP training in conjunction with a sensorimotor stimulation program can have benefits for motor restoration in the affected upper extremities of stroke patients. The experience of normal proprioceptive feedback and neurophysiological adaptation through repetitive bilateral movement practice can help restore patients' motor capability in affected upper limbs. Chen et al. [46] compared the improvements in motor impairment and functional performances of people with stroke after BULT and Unilateral Upper Limb Training (UULT) and found that BULT was superior to UULT in terms of improving motor impairment after a stroke, as measured by the Fugl-Meyer Assessment of Upper Extremity (FMA-UE).

Considering current trends such as system portability, lightweight exoskeletons, the advantages of the RTBP and the use of biomedical signals, this paper presents the integration of a five-finger exoskeleton, a system for the acquisition and classification of EMG signals, a fuzzy logic controller, and a graphical user interface (GUI) for robotic-assisted rehabilitation therapy with bilateral approach. The target users are individuals with the right hand affected by an accident or cerebrovascular problems which require passive or assisted rehabilitation. The left hand is considered as healthy, and its EMG signals are used to indicate the movements the exoskeleton must carry out to assist the paretic hand to complete the rehabilitation motion. Unlike other studies in literature which reported results for a reduced number of users, in this work an EMG signal database containing the results for 225 subjects (146 male and 79 female) for three essential movements with everyday activities (a total of 675 tests) is used for training and proving the classification algorithm using k-Nearest Neighbors (kNN). An accuracy of 81.2% was obtained, however, the influence of the random sEMG sensors alignment with regards to the muscles was reduced. A GUI was developed using Matlab software to provide a friendly interaction between the exoskeleton and the user by allowing bidirectional communication to occur. Performance tests were carried out by comparing the exoskeleton motion with the measurements of healthy person's hand movements. The obtained results are presented and compared to the data reported in the literature. The article is organized as follows. Section 2 describes the mechanical system and the redesign process for the construction of a second prototype based on a previous version. This section also describes the process and algorithms used for the exoskeleton instrumentation and control system. In Section 3, the results obtained from the control applied to the exoskeleton are presented. The measurements were obtained with a motion capture system and the results are based on the precision of the desired position. Section 4 discusses the results obtained in this study when compared to other investigations reported in literature. Finally in Section 5, conclusions about the integrated system and some proposed future tasks are provided.

2. Materials and methods

2.1. *System overview*

The exoskeleton was designed for bilateral rehabilitation. This rehabilitation strategy is based on natural coordination between the healthy limb and the affected limb, thereby improving the efficiency of the grasping movements on the affected side. Bimanual tasks require the coordinated work of both hands so that they cooperate to achieve the desired function [47]. Activation of the primary motor cortex and supplementary motor area (SMA) of the healthy limb increases the probability of voluntary muscle contractions in the damaged limb when performing symmetrical movements [48]. The simultaneous movement of both limbs helps the neuromuscular system to regain stability and improves the use of the affected limb, including grasping tasks. In order to reproduce this type of therapy, the exoskeleton must be placed on

the user's affected hand and reproduce the movement that the user makes with a healthy hand [49].

The complete system is comprised of 5 main subsystems: motion detection, motion classification, desired reference assignment, controller and the exoskeleton. The system operation begins with the use of the MYO armband on the user's left arm, to detect when a movement is made, by acquiring EMG signals. A data set had been previously created to train the learning algorithm that determines the type of movement the user is making in real time. When the movement is identified, a value is assigned to the desired positions of each motor. These desired positions are obtained beforehand through a motion capture system by determining the path of each phalanx to perform a certain hand gesture. When the path is assigned, the DC motors which drive the movement of the exoskeleton's fingers are activated, and by means of the control system action the reference must be followed. Fig. 1 shows the general block diagram of the whole system.

2.2. *Mechanical system*

The mechanical design of the exoskeleton used in this work was previously reported in [50]. For the integration of the instrumentation and control system, some parts of the exoskeleton were redesigned, in order to increase strength and functionality, reduce general dimensions and improve the aesthetic appearance. To corroborate the position of the actuators in relation to the centers of rotation of the fingers, a motion capture system was used. A large part of the prototype was made based on 3D printing by Fused Deposition Modeling (FDM), facilitating the easy reproduction and redesign of components for future users or research.

2.2.1. *Hand gestures description*

Abduction and flexion movements of the thumb are important for the natural reproduction of a healthy hand's movements, as the manipulation of large objects is made easier by the support from the palm of the hand and small objects from the fingers. There are currently several studies reported in the literature providing anatomical information and the dynamic role that the thumb performs during the development of hand movements as pointed out in [51,52]. This concern for the implementation of thumb mechanics has been transferred to grip technology, as it allows the execution of pinch grasps [53]. In our proposed design, abduction movement of the thumb is not possible. However, this issue does not limit the exoskeleton's mobility for carrying out the three hand movements considered in this work (fist, cylindrical grip and tip pinch). Taking this into account for the prototype design, the movements that the exoskeleton reproduce were characterized by a motion capture procedure which obtained specific ranges of movement of each finger in the different grasping tasks. This technique generated reference values to evaluate the development of the prototype in the final tests and the precise location of the interphalangeal joints, for the redesign of the exoskeleton.

The fist, cylindrical grip and tip pinch movements were studied in this work. These movements are those performed by a healthy hand and are essential for carrying out different activities in everyday life. The selection of movements was made based on the movements reported for a rehabilitation therapy [54]. For the cylindrical grip exercises the user grasps a plastic cylinder with a diameter of 8 cm and a length of approximately 12 cm. For the tip pinch the user picks up a commercial marker with the pad of the thumb and index finger. For the fist, the user only closes the fist and keeps it in that position until the test ends.

2.2.2. *Design specifications obtained by motion capture*

Motion capture is a process that uses equipment that is able to capture and determine the location of points in a body of a user in a given period of time [55]. The points detected by the camera are reflective marks which are then processed to obtain kinematic information. For this work, the Vicon™ system composed of 8 Bonita infrared cameras was used. The software to perform motion capture and data collection is called Nexus®, with the generated and processed information available to export as an Excel file for manipulation by another mathematical software.

Different tests were performed for each of the above-described movements. The position of the marks on the index finger and thumb is shown in Fig. 2 for a cylindrical, fist move-

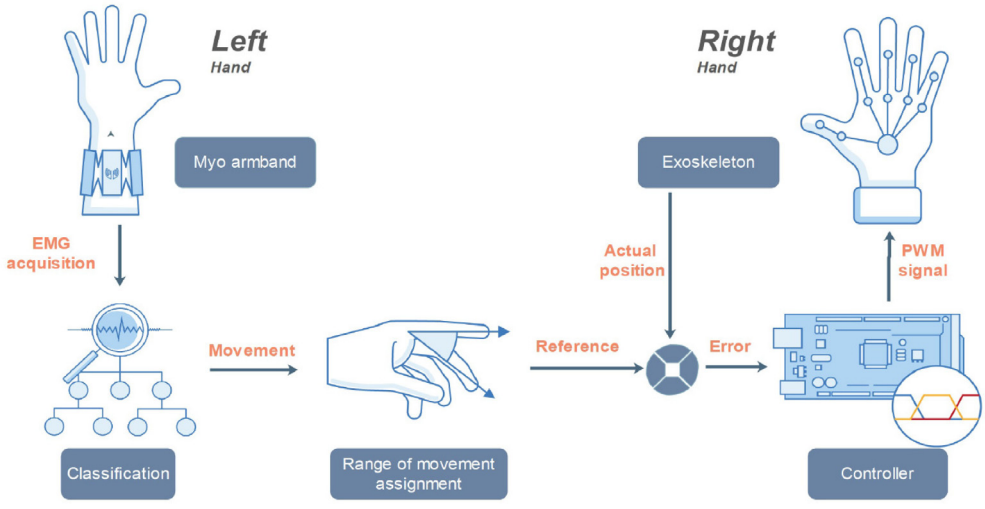


Fig. 1 – System block diagram.

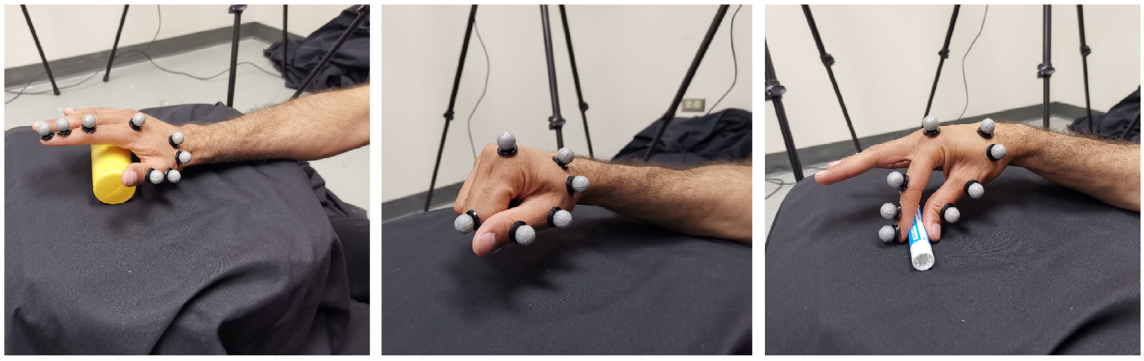


Fig. 2 – Location of marks for the motion capture system test. a) Cylindrical grip. b) Fist. c) Tip pinch.

ment and tip pinch. The marks are small spheres that were placed at the termination of the distal phalanx and the distal interphalangeal, proximal interphalangeal, metacarpophalangeal and carpometacarpal joints of the index to the little finger. For the thumb, the marks were placed at the distal interphalangeal, metacarpophalangeal and carpometacarpal joints. A further mark was placed at the base of the bench which functions as a reference mark for further kinematic analysis. Different tests were performed for each of the fingers, and the resulting test data are available in [56]. During the preparation of the tests, the positioning of the cameras and the creation of kinematic chains in Nexus software is essential, otherwise confusion regarding the marks or loss of data may occur during the test.

In this project, the files generated by the software were exported to Matlab for kinematic analysis. Each test contains information about the marks position in the XYZ space during the time period the test data were acquired. Fig. 3 shows the position of the index finger marks for a fist test. To obtain this visualization, a mark placed at the base of the bench was taken as a pivot. The positions of the following marks were obtained through rotation matrices.

Rotation and translation matrices were applied to the point cloud, based on the data from the mark on the carpometacarpal joint. The analysis was carried out individually for the five fingers. The result of this analysis is the angular range of movement that each of the phalanges must develop as well as the trajectory that the exoskeleton should follow. The rotation matrices used are described by the following equations:

$$R_{x,\phi} = \begin{pmatrix} 1 & 0 & 0 \\ 0 & cos\phi & -sen\phi \\ 0 & sen\phi & cos\phi \end{pmatrix} \quad (1)$$

$$R_{y,\theta} = \begin{pmatrix} cos\theta & 0 & sen\theta \\ 0 & 1 & 0 \\ -sen\theta & 0 & cos\theta \end{pmatrix} \quad (2)$$

$$R_{z,\psi} = \begin{pmatrix} cos\psi & -sen\psi & 0 \\ sen\psi & cos\psi & 0 \\ 0 & 0 & 1 \end{pmatrix} \quad (3)$$

The results obtained for the cylindrical grip were compared with the values reported in [57]. The cylinder used in this project has a diameter with a value between the two diameters value of the objects reported in the experiments of [57], however, by means of interpolation it was confirmed that the results of both experiments are similar. Fig. 4 shows the references for measuring the angles representing the angular motion of the different finger joints of three different

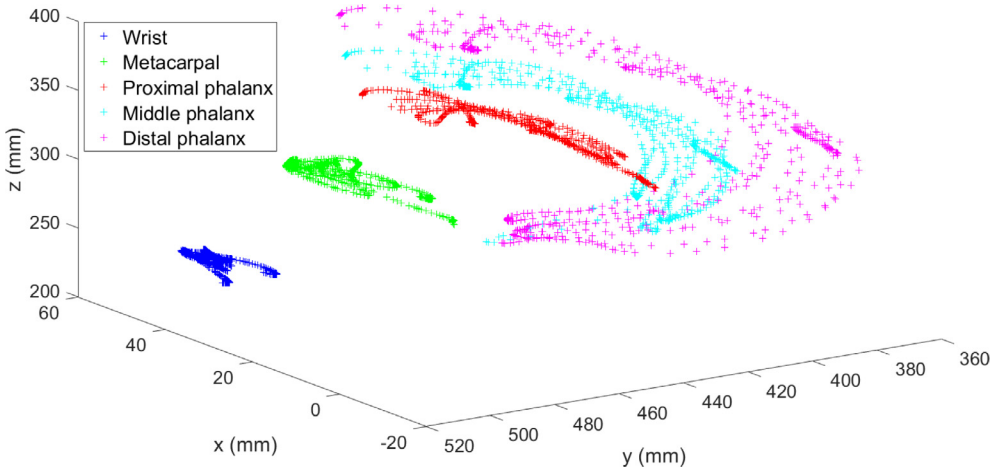


Fig. 3 – Positioning of the marks in the XYZ space for the cylindrical grip.

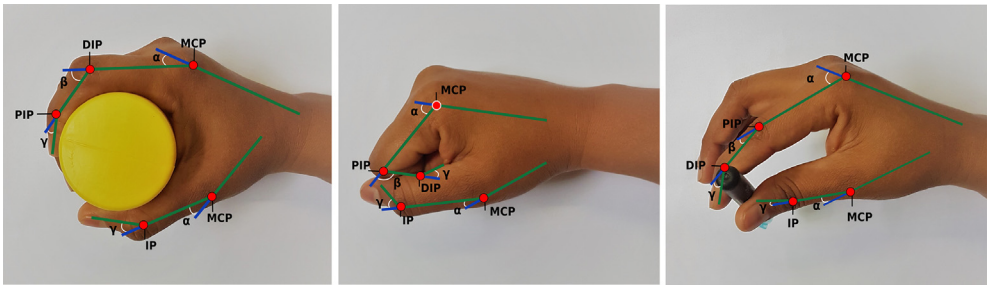


Fig. 4 – Graphical representation of the angular movements of the different joints of the hand for a) Cylindrical grip, b) Fist, and c) Tip pinch.

hand movements. Angle (α) representing the movement of the metacarpophalangeal joint (MP) is obtained as a result of the angle delimited by the prolongation of the metacarpal bone and the proximal phalanx. Angle (β) representing the angular movement of the proximal interphalangeal joint (PIP) is obtained as a result of the angle being delimited by the prolongation of the proximal phalanx and the middle phalanx. Angle (γ) representing the angular movement of the distal interphalangeal joint (DIP) is obtained as a result of the angle delimited by the prolongation of the middle phalanx and the distal phalanx. The values of these angles are shown in Table 1 for three different hand movements.

2.2.3. *Mechanical structure and actuation system*

The exoskeleton was designed with the aim of solving the problem of tracking the center of rotation of the phalanges without mechanical interference with the user's fingers. Regarding the finger movement, the location of the phalanx's center of rotation changes. A gear and rack mechanism was chosen to cover the full range of motion of each of the five fingers' phalanges. The ring, middle and index fingers can move independently of the proximal and middle phalanx. The thumb and little finger can only move due to the proximal phalanx. Because of this design, the exoskeleton has one motor per movement block with a total of 8 DC motors for

Table 1 – Ranges of movements for three basic hand movements (degrees).

Movement	Phalanx	Thumb	Index Finger	Middle Finger	Ring Finger	Little Finger
Fist	Proximal (α)	54.108	38.623	60.235	33.145	54.108
	Middle (β)	–	82.701	79.852	87.430	62.980
	Distal (γ)	62.980	81.397	76.847	81.397	83.412
Tip pinch	Proximal (α)	54.813	54.813	61.447	58.656	54.813
	Middle (β)	–	45.199	45.513	50.840	45.199
	Distal(γ)	50.363	50.363	52.913	50.840	50.363
Cylindrical Grasp	Proximal (α)	35.230	17.825	2.020	1.980	1.950
	Middle (β)	–	49.176	3.020	3.450	3.380
	Distal (γ)	44.980	37.229	2.980	2.980	3.020

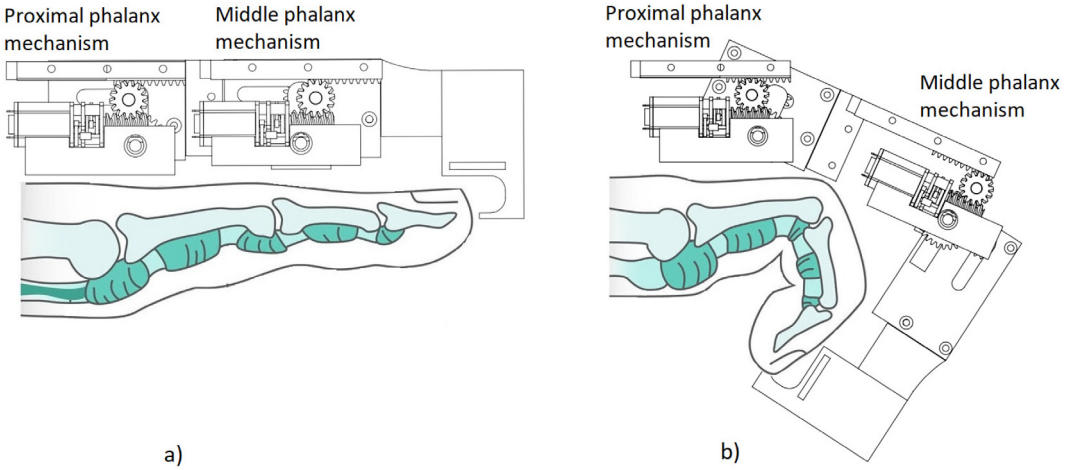


Fig. 5 – a) Side view of a finger of the exoskeleton. b) Finger of the exoskeleton during the flexion movement.

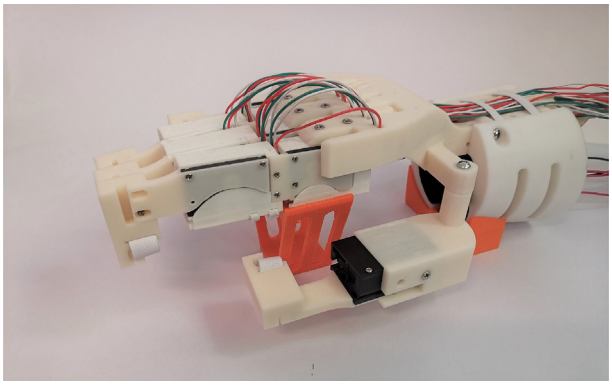


Fig. 6 – Final assembly of the prototype.

independent movement of the fingers, while the finger mechanism consists of two blocks. The first block performs the movement of the proximal phalanx and is attached to the base of the exoskeleton while being supported on the metacarpal bone. The second block performs the movement of the middle phalanx and rests on the proximal phalanx. Fig. 5a) shows a side view of the new design of a finger mechanism with the location of the blocks. Compared to the previous version of the prototype reported in [50], the new design completely covers the internal components of the main mechanism during the movement, avoiding contact by the user towards the elements for power transmission.

Each of the movement blocks has two gear-rack sets. One of the sets is responsible of the rotational movement and its transmission to the next block, while the other set handles linear scrolling. In this way, it is possible to keep the device coincident with the centers of rotation of the fingers. Each of the blocks contains a Pololu DC motor with a 150:1 gear ratio. A worm-gear mechanism was used to transmit power from the motor to the mechanism, as depicted in Fig. 5a). Fig. 5b) shows the exoskeleton carrying out the finger flexion movement. In this position, the motion of each finger phalanx conduced by each block of the exoskeleton mechanism can be clearly observed. For the dimensioning of the mechanical elements, the data reported in [58] were used. For details of the parameter calculations and dimensioning of the pieces, the previously procedure reported in [50] was followed. Firstly, 3D printing was used for the construction of the second prototype due to the many advantages that this technology offers. The power transmission spur gears from the motor were made of 1060 Aluminum, while the rest of the exoskeleton parts were printed in PLA. The main base that is placed on the hand and that holds the fingers was redesigned with guides for the cables coming from the encoders. The bases were covered with a quilted cotton fabric to avoid discomfort to the user. Fig. 6 shows the final assembly of the exoskeleton, showing the cables for the connections between the drive and signal acquisition systems.

The total weight of the exoskeleton is 730 g including actuators, as well as mechanical and electrical parts. Each movement block consists of 16 pieces while an average time of 52 h is required to print the entire skeleton. The device can be adjusted for different hand sizes and finger length by using guides that are adjusted by screws to extend or shorten of the mechanism's length. The fingers move independently with a range of 0–90° and 0–110° for the proximal and middle phalanges, respectively.

2.3. *EMG signal acquisition and classification system*

The development of the exoskeleton control system is oriented to assisted rehabilitation therapy. The patient's willingness to be active is required during the entire movement with the exoskeleton providing weight or force support in order to complete the task [59,60]. For this therapy approach it is necessary to know the user's intention, and one way of doing this is through electromyographic (EMG) signals. The MYO armband was used for EMG signal acquisition by reading the muscles' electrical activity with its 8 sensors which are then transmitted to the computer using Bluetooth technology [61]. Fig. 7 shows the block diagram of the process for detecting movement, the offline training and the online implementation. Each of the tests lasted 5 s, which is enough time to obtain information on movement without the user suffering from fatigue.

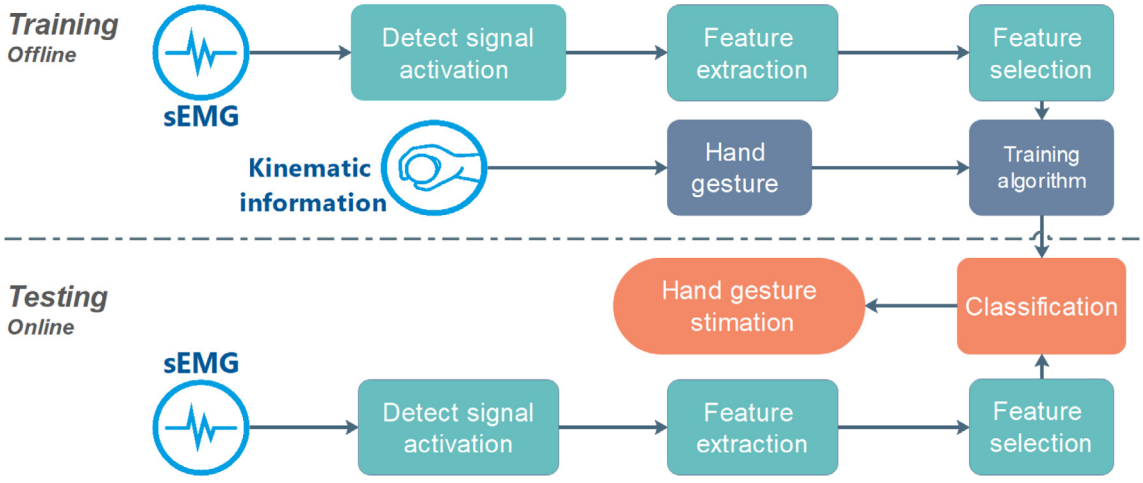


Fig. 7 – Block diagram of the classification process. Offline training and online testing.

2.3.1. Acquisition and processing of EMG signals

To train the classification algorithm, a database was created with 225 tests for each movement, with each test corresponding to a different subject. All tests were performed on the arm of the non-dominant hand, and the database is available for free download at [62]. During the sampling time of the test, there is a delay at the beginning while the user starts to carry out the movement which is considered as a noise. To detect the muscle activity, an algorithm based on the evolution of the signal over time using a combination of energy and zero crossings was implemented as shown in Eq. (4).

$$C = \sum_{m=0}^{L} |x[m] \cdot |x[m]| - x[m-1] \cdot x[m-1]| \quad (4)$$

Eq. (4) is comprised of the mathematical formulation of the Zero Cross Density, while the sign functions are multiplied by the Energy of the analyzed sample. Therefore, the accumulated density depends on the change of sign of the samples and their amplitude, meaning that the noise does not result in an accumulation of density [63].

Subsequently, the signal is rectified and filtered with a Butterworth low pass filter. The next step was the extraction of signal features [64] and the features extracted from the signal were: Waveform Length, Mean Absolute Value, Root Mean Square, Variance, Kurtosis, Zero Crossing, Willison Amplitude, Slope Sign Change, Entropy, and Average power. In total, for each test taken 80 features were obtained, this is the result of 10 features for the 8 EMG sensors on the MYO armband.

2.3.2. Classification of EMG signals

A large number of features does not guarantee the classification algorithm's accuracy, and it is important to use the most relevant features in each movement [65]. The reduction of the original set must be carried out under an evaluation criterion known as selection of characteristics. For the generated database, different data subsets were obtained with the algorithms Sequential Forward Selection (SFS), Sequential Floating Forward Selection (SFFS) and Random Subset Feature Selection (RSFS). These algorithms were selected due to their speed of convergence, higher learning accuracy and lower computational cost [66]. The SFS algorithm starts working from an empty set Y_0 and the best feature is added to this set. The feature x^+ gives the highest correct classification rate $J(Y_k + x^+)$ which is then added to $Y_k$at each step along with the features which already included in Y_k. The process continues until the correct classification rate given by Y_k and each of the features not yet selected does not increase [67]. The SFS algorithm performs the following steps:

1. Start with the empty set Y_0
2. Select the next best feature $x^+ = argmax_{x^+ \notin Y_k}[J(Y_k + x^+)]$
3. If $J(Y_k + x^+) > J(Y_k)$
   3.1. Update $Y_{k+1} = Y_k + x^+; k = k + 1$
   3.2. Go to step 2
4. End

One of the problems with the SFS method is that once an element has been added it cannot be removed. SFFS permits the removal of previous features added to the subset. It does this by initially working from an empty set Y_0 and in each step a new subset is generated first by adding a feature x^+. However, after this step the features x^- is identified in order to be eliminated from Y_k until the correct classification rate $J(Y_k - x^-)$ decreases. The iterations continue until no new variable can be added because the recognition rate $J(Y_k + x^+)$ does not increase. The SFFS algorithm performs the following steps:

1. Start with the empty set Y_0
2. Select the next best feature $x^+ = argmax_{x^+ \notin Y_k}[J(Y_k + x^+)]$
3. If $J(Y_k + x^+) > J(Y_k)$
   3.1. Update $Y_{k+1} = Y_k + x^+; k = k + 1$
   3.2. Remove the worst feature $x^- = argmax_{x^- \in Y_k}[J(Y_k - x^-)]$
   3.3. If $J(Y_k - x^-) > J(Y_k)$
      3.3.1. Update $Y_{k+1} = Y_k - x^-; k = k + 1$
      3.3.2. Go to step 3.2
   3.4. Else
      3.4.1. Go to 2
4. End

This algorithm is based on the idea of Random Forests and Random k-Nearest Neighbors (kNN). It selects a set of features that work better than an average feature of the available feature set. The most relevant feature set is obtained by repetitively choosing a random subset of features from the set of all possible features and then sorting the data with a kNN classifier [68]. During each iteration, the relevance of each feature is adjusted according to the performance of the subset classification in which it participates. Each characteristic is evaluated in terms of its average utility in the context of many other combinations of features. During each iteration i, the RSFS algorithm performs the following steps [68]:

1. Randomly select a subset S_i of n features $f_x(|S_i| = n)$ from the full set F by sampling from a uniform distribution.
2. Perform kNN classification on the given data set using S_i and computes the value of a desired criterion function c_i which measures classification performance.
3. Update relevances r_j of all used features f_j by replacing them with
$$r'_j = r_j + c_i - Ec \quad (5)$$
4. Repeat the process from (1) with a new random subset.

The algorithms described above were implemented in Matlab. A subset of 9 features were obtained by the SFS algorithm, 16 features by SFFS and 30 features by RSFS. The results and the procedure are described in more detail in [69]. The obtained subsets were used to train four classification algorithms. Moreover, the machine learning techniques employed were Support Vector Machine (SVM), k Nearest Neighbors (kNN), Linear Discriminant Analysis (LDA) and Decision tree learning. Table 2 shows the accuracy results of each of the algorithms with the different subsets of features.

The selection of the subset feature has a major impact on the final performance of the classification algorithms, both positively and negatively. For example, in Table 2 can be seen

Table 2 – Accuracy results for different classification algorithms (%).

Feature selection algorithm	Classification algorithm			
	kNN	SVM	LDA	Decision tree
SFS	67.1	74.2	71.0	71.3
SFFS	69.9	75.3	73.8	71.6
RSFS	81.2	77.5	76.0	74.1
Without	74.1	73.6	69.3	70.8

that kNN with the entire group of features has a better performance than when SFS and SFFS is applied. This is because the feature subsets do not fully describe all classes. Due to the nature of the algorithm when receiving a new data to classify, it takes the closest or neighboring data of it, however, these do not correspond with the features of the real class. With regards to the RSFS, each feature is selected depending on its performance when it is evaluated within different subsets. This is in contrast to the SFS and SFFS where each of the features is directly included or excluded from the final subset of features. Therefore the relevance of the RSFS is adjusted because of the influence it has on various random subsets. It is for this reason that RSFS has a lower probability of converging to locally optimal solutions. It is possible to visualize this fact with the results shown in Table 2 where for the four classification algorithms, the best result is obtained by applying an RSFS selection. Although not everything depends on the features selection, the behavior of the classification algorithms is an important factor regarding performance. In contrast to kNN, SVM makes a separation by hyperplanes where each new data to be classified is evaluated for its membership to each group. Therefore, when SFS and SFFS are used with SVM, its performance is improved.

In Table 3 a comparison of different issues from our proposal with other EMG signal classifiers is presented. Most of the mentioned works report classification results based on only a few numbers of test subjects, while the results reported in this work consider 225 test subjects with an accuracy of over 80% which are in the range of the results reported in Table 3 (from 67% to 98%). As previously mentioned, the performance of the EMG signals classifier can be strongly affected by the variation in the placement of EMG sensors and this effect can be reduced by using a large database as proposed in this work.

2.4. *Control system*

2.4.1. *Design of the fuzzy controller*

In the literature, a variety of control techniques can be found, including classical ones such as Proportional Derivative (PD) control, Proportional Integral Derivative (PID) or other more modern techniques that improve the system's response such as the Linear Quadratic Regulator (LQR) controller or Sliding Modes (MD). The application of PID controllers has been car-

Table 3 – Performance comparison of classifiers for different body movements with diverse number of test subjects.

Reference	Classifier	Accuracy	Number of subjects	Identified motions	Sensor location
Our proposal	kNN-RSFS	81.2%	225	Cylindrical grip, fist, tip pinch	Forearm
[22]	Multiclass SVM	98%	6	Shoulder retraction/protraction	Shoulder
[23]	SVM	97%	5	Elbow flexion/extension	Forearm
[24]	SVM	93%	62	52 hand movements	Forearm
[25]	PSO-PVM	97%	27	Elbow flexion	Arm
[26]	ANN	98.7%	12	Double tap wave in/out, fist	Forearm
[28]	SVD-WDBN	83.8%	8	Shoulder and elbow flexion/extension, fist	Shoulder, arm and forearm
[29]	LDA-kNN	71.17%	9	Wrist, thumb, index flexion, fine pinch fist	Arm
[31]	kNN	88%	25	Not specified	Arm
[32]	kNN	94%	13	Fist, thumb and index flexion/extension	Arm
[34]	RF	Not specified	6	Walk back and forth	Leg
[37]	ANN, SVM, kNN	98%	20	Thumb, index flexion, closed hand	Forearm
[40]	HRM	98%	4	Open hand, fist spherical grip	Forearm
[41]	ADANN	81.38%	22	10 hand gestures	Forearm
[42]	ANN	67%	5	Wrist and elbow flexion/extension	Arm

ried out on different rehabilitation devices, the majority for the upper limb without covering the hand. The design and application of artificial intelligence-based control techniques such as fuzzy versions of PD or PID controllers are currently under development. Owing to the advantages offered by fuzzy controllers (e.g. no dynamical model required, robustness, flexibility [70,71]) a fuzzy PD control was implemented in the exoskeleton. The task for the controller was established as a tracking problem, where the references are the desired trajectory of each phalanx previously obtained by the motion capture technique. The system outputs are the measured angular positions of the exoskeleton joints. There are three stages to designing the fuzzy controller:

- FuzzificationFuzzy-type controllers have membership function set inputs, meaning that the input variables are linguistic-like. For this particular controller the linguistic variables are Error, Change, and Voltage, while the linguistic terms are negative, zero and positive for each variable. The fuzzy driver inputs are Error (e) and Change error (de/dt), and the error is defined as the difference between the desired angle and the actual angle. The range of values between which the error is defined are [-1,1], and at each encoder reading the error is updated and normalized. An error with a value of 1 means that the phalanx is at 0°. Additionally, the controller output is a value corresponding to the high cycle of the pulse width modulator (PWM), which controls the speed of the actuator. The functions that model the linguistic terms are trapezoidal. Due to the necessity of two PWM signals and nine input/output ports (GPIO) for every two motors, the controller was implemented on an Arduino Due development board where 8 PWM and 36 GPIO ports are used for motor drivers and encoders. In order to generate the PWM signal, it has to work with an 8-bit resolution [0–255] which is equivalent to 0–100% of the duty cycle. For the undertaking of the tests in this project, the maximum duty cycle to be generated by the card is 21%, since at this speed the motion capture system can acquire consecutive data without confusions between the marks.
- Fuzzy rules.Fuzzy rules are established to relate the inputs to the outputs, making combinations of the input groups, since there are two inputs with three linguistic terms each with nine rules needed. The implemented rules are shown with greater detail in the work presented in [72].
- Inference system.The inference method to be used for the fuzzy intersection is the Mandani method [73]. To obtain this phase, the Matlab software tool is used, with the help of the fuzzy logic toolbox.

2.4.2. *System integration*

In order to communicate the computer with the exoskeleton, an Arduino development board acquires the pulses per revolution from the encoder and generates the PWM signal. Several factors were considered when selecting this platform such as: the number of pins available, the number of PWM pins, processing capacity, programming language and memory. An Arduino Due board was selected, as the Due version of the Arduino has 14 PWM and 54 GPIO pins. The control of the DC motors is carried out on the board, while the fuzzy system was created in this same language with the parameters and tuning of gains obtained from Matlab. To control the motors and receive information from the encoders, a printed circuit board (PCB) that connects to the Arduino and the drivers was designed. This PCB provides the necessary ports for communication and power supply of the exoskeleton. The Arduino receives the values that each of the motors must reach as the reference values from Matlab through serial communication. During each iteration the position of the motor is updated through information from the encoders, and the values of error and the change of the error are obtained. In order to deduce the PWM signal to be generated by the Arduino, the values are updated in each iteration by means of defuzzification of the fuzzy system. When the fuzzy controller reaches the desired values, the system pauses for 6 s to resume the movement of the motors, but now in reverse and to return the phalanges to the initial position. The exoskeleton's internal motors are connected to a data acquisition card for data transmission to a computer. The computer receives the signals from the MYO armband and they are recognized in the graphical user interface.

- Computer for signal processing
- Mechanical system
- Control and data acquisition system
- Instrumentation system
- Test grip elements (plastic cylinder and down)

2.4.3. *Design of a Graphical User Interface (GUI)*

A graphical user interface (GUI) was developed to provide a user friendly interaction between the exoskeleton and the user. The developed GUI receives the EMG signals and sends the references for each of the exoskeleton's phalanges without a user interference during the undertaking of the process. The guidelines established during the GUI design process were to have clear and concise texts and graphics, colors commonly used in the medical area, intuitive menus, integration of all subsystems and presentation of the elements in an accessible way. The requirements of this type of systems must be proposed based on usability concepts in order to design a system that user friendly and easy to learn. Three concepts must be considered during the design to achieve this goal: satisfy operating requirements, complete tasks effectively and make the user feel comfortable when interacting with the interface.

In accordance with the established requirements, the graphical interface was developed in Matlab, because the processing and classification of the signals are carried out using this software. A screenshot of the developed GUI is shown in Fig. 8 and is divided into four main sections.

- Execution: In this section there are two options: Start and Stop. When the user presses the Start button, the system begins execution with the acquisition of the EMG signals and movement of the exoskeleton.

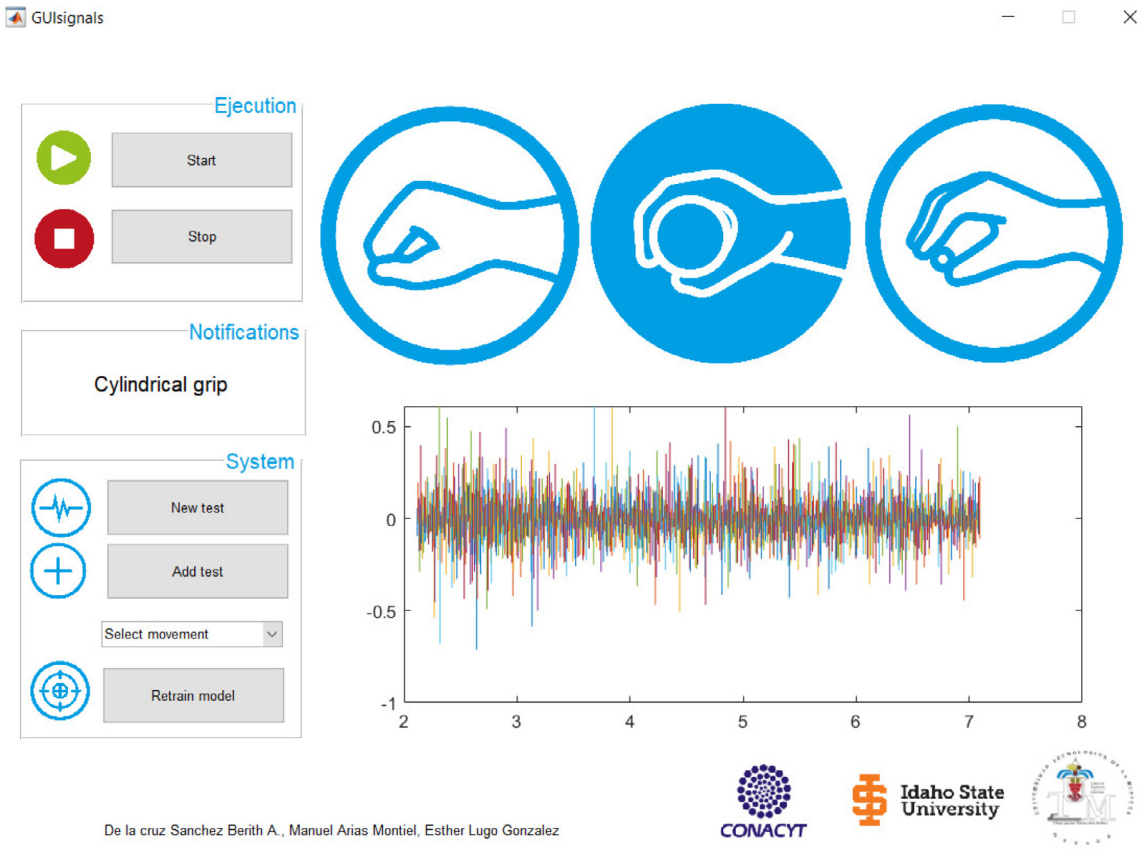


Fig. 8 – Main view of the Graphical User Interface.

- Notifications: During the execution of the application, different messages are displayed to guide the user. For example, a warning appears when there is gripping, periods of rest and when the exoskeleton's movements start and finish.
- System: It is possible to add a new test to the database and recalibrate the classification algorithm, incorporating new data into the system thereby making it more robust.
- Graphics: In this section the three movements that the system reproduces are shown. An icon changes color depending on the movement that is detected, while the graphics of the acquired EMG signals are shown in this section as well.

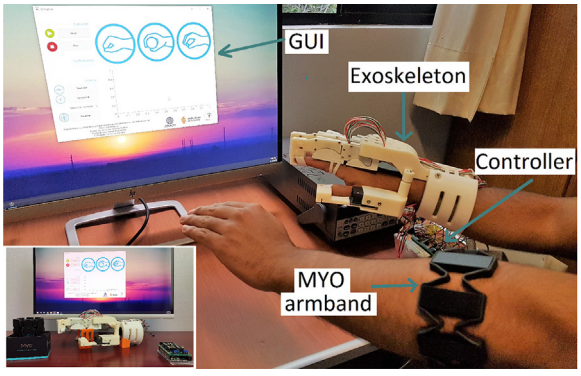


Fig. 9 – General view of the complete system.

In order to start a new test only the "Start" button needs to be pressed, and the system will show different legends in the notifications section. The system starts by loading the MYO armband's libraries, and when it is ready to start data acquisition, a notification is displayed for the user to perform a hand movement. The data acquisition period lasts 5 s, and once acquired, the sample conditioning process begins. The signal is trimmed to detect muscle activation, filtered, normalized and its characteristics are extracted with which the membership will be evaluated. When the system produces a result, the colors are inverted to the figure corresponding to the movement in the graphics section. Fig. 8 shows the main screen of the program when a cylindrical grip movement is detected, and the figure with the cylindrical grip is highlighted. It is possible to press the "Stop" button at any time which stops the system, whereby the application closes and if the exoskeleton is in motion, it stops. An overview of the elements of the system is shown in Fig. 9.

3. Results

The tests to analyze the performance of the system were carried out with the authors of this article. The EMG signals were obtained from the authors' left hand and the exoskeleton placed in the right hand replicated the movement. Fig. 10 shows the final position of the exoskeleton for a fist-lock and cylindrical grip test.

To assess the exoskeleton's performance, tests were performed with the motion capture system, with marks placed on each of the exoskeleton's phalanges as shown in Fig. 11 a). While Fig. 11 b) shows a general view of the scenario where the tests were performed, the user was positioned in the center of the room to cover the different planes with the cameras. Due of the size of the marks, there is the possibility of confusing the system and collecting erroneous data, therefore, the tests were carried out with each one of the fingers. The exoskeleton was placed on the hand of a healthy person and the measurements were obtained with reference to a mark located on the wrist. During the tests, the mark located on the wrist was the reference for the system's calibration.

After collecting the test results for each of the fingers of the different movements, the trajectory analysis was performed in Matlab. The data were conditioned with rotation matrices to compare the results obtained from the exoskeleton's movement and from the healthy hand. One way to visualize the range covered by the exoskeleton of each of the movements is to plot both trajectories, as shown in Fig. 12. The plot shows the path that the exoskeleton's index finger should follow to perform a fist and cylindrical movement. The curves for each of the phalanges are shown in a different color. Similarly, this analysis of the results was performed for the hand's five fingers with the three different grips.

The three movements for the middle finger are shown in Fig. 13. The results of the index and middle finger are presented because during the fine gripper movement they have a different range of motion.

The movement curves of the exoskeleton are very similar to that of the finger, which serve as a reference in the controller. The error was calculated based on the measurements obtained with the motion capture system, considering as a reference the final position to which the exoskeleton should arrive and which are defined by the data from Table 1. Table 4 shows the error for each of the fingers' phalanges when performing the proposed movements. The data are reported in percentage of error, where the smallest value is the closest to the reference value.

To obtain the error of each of the phalanges, several tests were carried out on each of the fingers, and the average for the measurements obtained are those reported in this document. The maximum observed error is 10.63% and the mini-

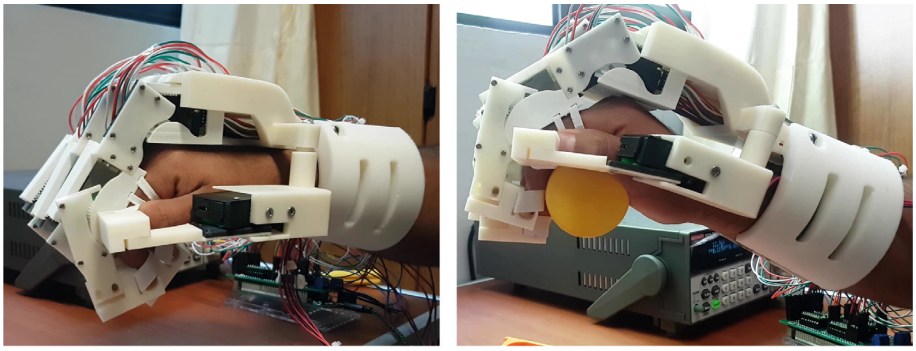


Fig. 10 – Final position of the exoskeleton: (a) fist-lock and (b) cylindrical test.

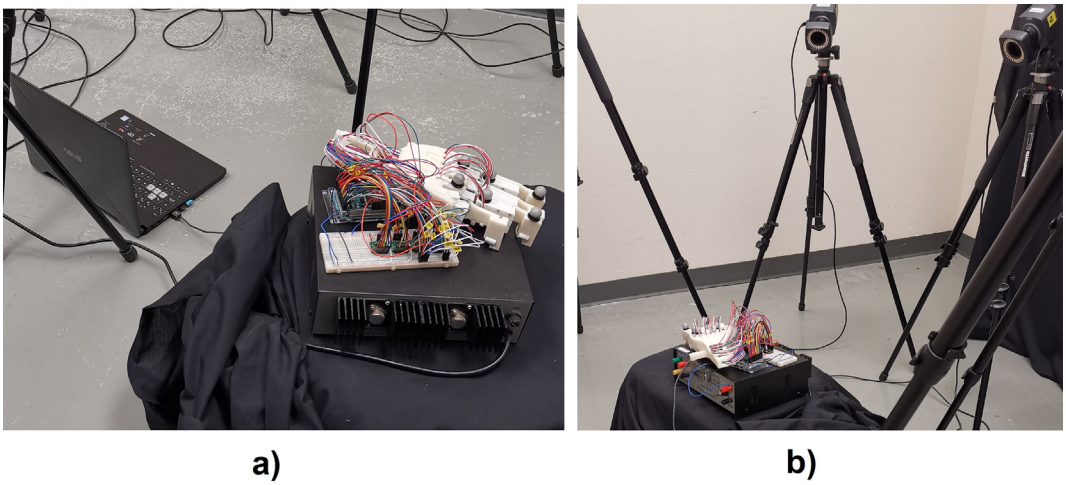


Fig. 11 – Prototype motion testing with MOCAP. a) Exoskeleton with marks used with the motion capture system, b) Motion capture scenario.

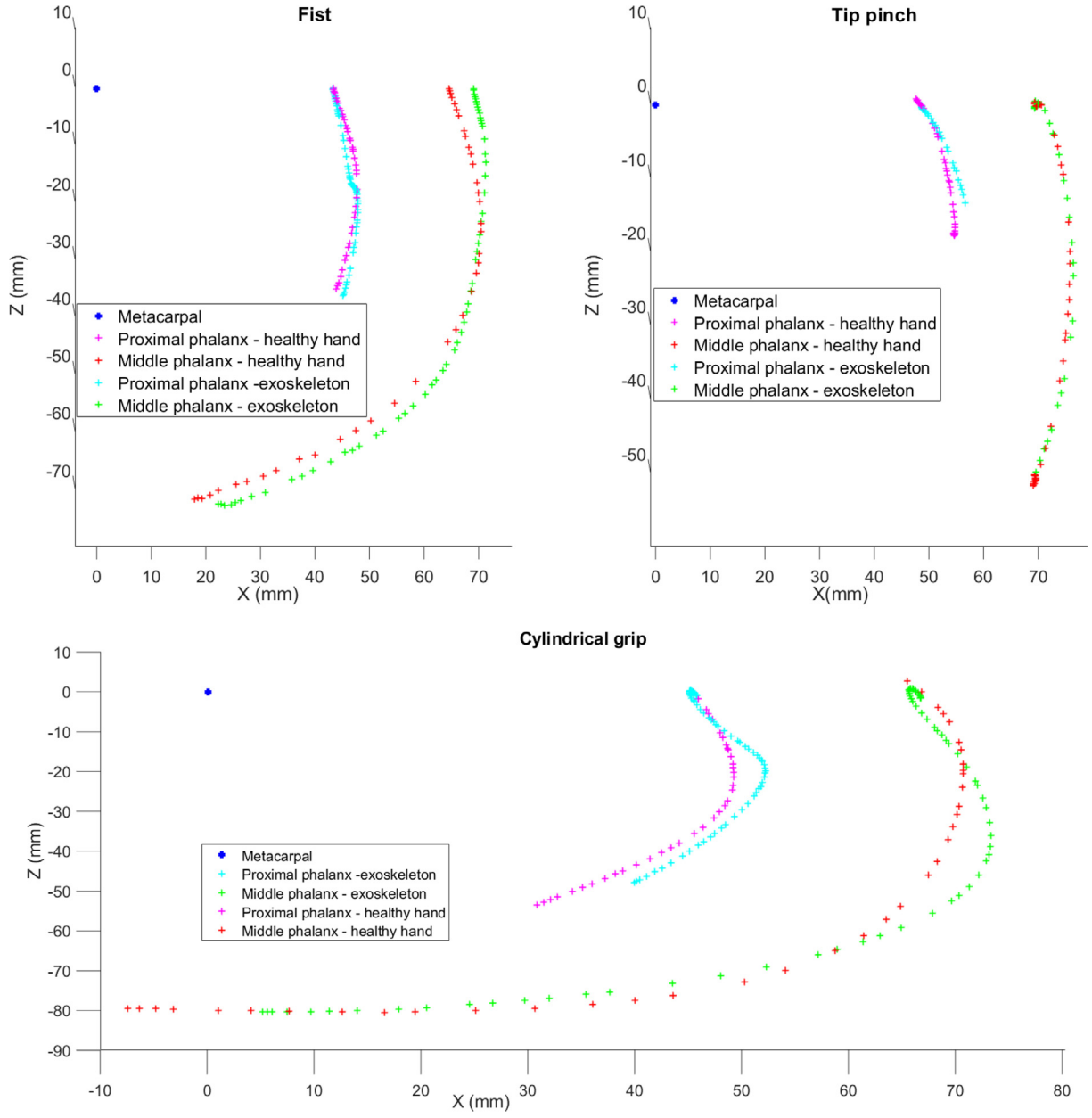


Fig. 12 – Comparison of results obtained from the exoskeleton and the ranges of movement of a healthy hand for the index finger in fist, tip pinch, and cylindrical grip movement.

mum is 3.46%. In terms of angular movement, this is equivalent to a difference of 1.89° and 0.07°. For each test both of the user's hands were involved. The MYO armband was placed on the left arm, while the hand's movement was carried out with the right arm, assisted by the exoskeleton.

The most significant errors occurred when undertaking small movements, and the results obtained are strongly influenced by the mechanical system due to the tolerances considered for assembly. This error is also caused by the margin of error that exists in the control compared with the desired value in the motors that receives a signal of zero PWM. If the response time and processing of the Arduino development board reduces the margin, the motors start to oscillate on the desired value without being able to establish itself. To avoid this, the range in the PWM signal with a 0% of duty cycle is extended. Currently, this margin of error is visually imperceptible visually which is also the case regards to therapy. However, it can be reduced with the application of the control system in another development board with a greater processing capacity along with improved actuators.

4. Discussion

The results in Table 4 show that the exoskeleton successfully reaches the desired positions for all three types of grip. One of the disadvantages of the exoskeletons reported in the litera-

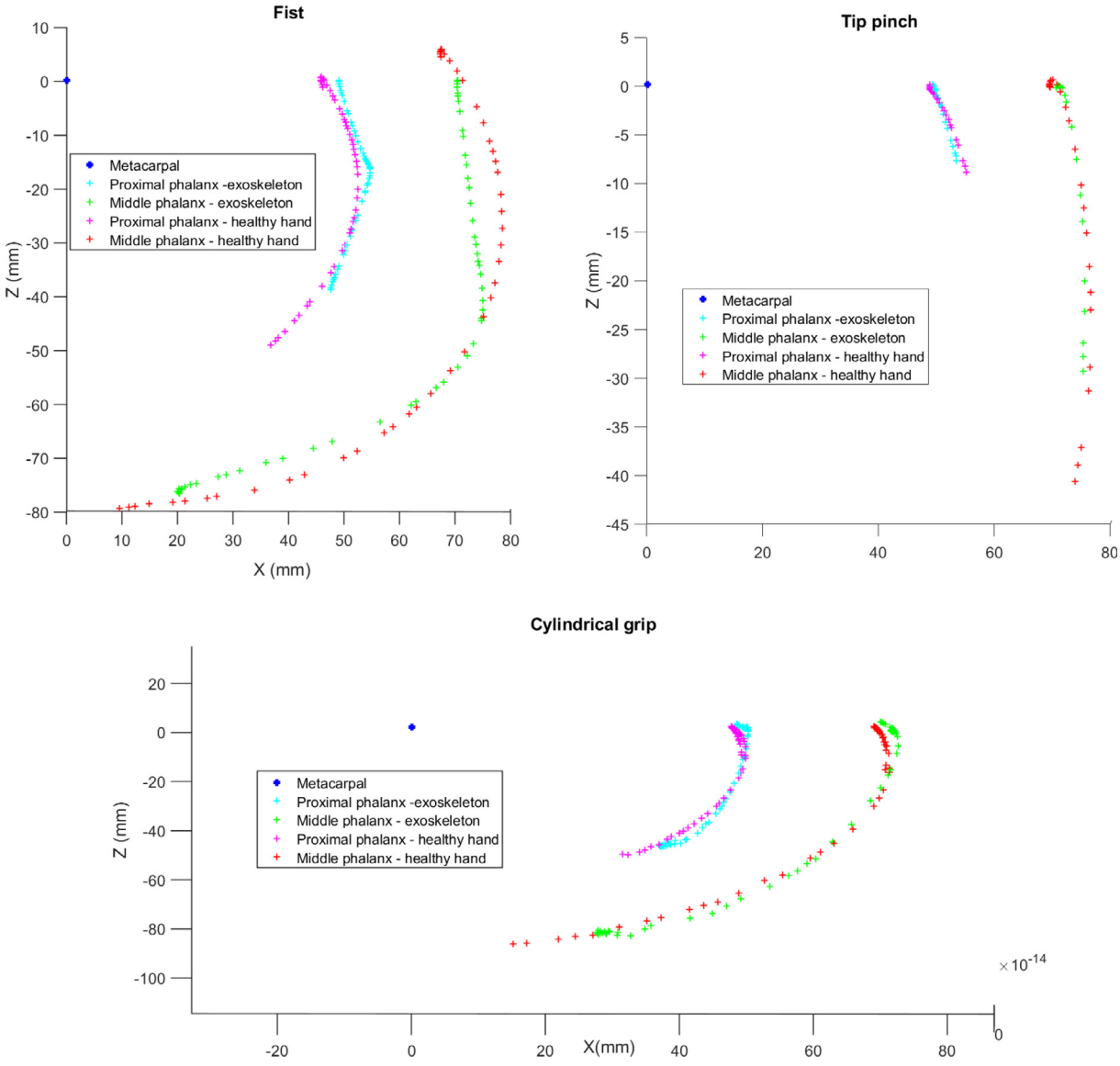


Fig. 13 – Comparison of results obtained from the exoskeleton and the ranges of movement of a healthy hand for the middle finger in fist, tip pinch, and cylindrical grip movement.

Table 4 – Global movement errors with the exoskeleton placed on the hand (%).

Movement	Phalanx	Thumb	Index Finger	Middle Finger	Ring Finger	Little Finger	Total
Fist	Proximal	7.57	7.89	7.03	9.49	7.59	7.91
	Middle	9.42	6.89	7.07	7.20	8.42	7.80
Tip Pinch	Proximal	7.32	6.93	5.96	6.55	6.50	6.652
	Middle	6.67	7.07	7.06	6.24	6.25	6.658
Cylindrical	Proximal	8.17	10.63	3.46	6.56	3.58	5.76
	Middle	7.89	7.40	5.71	3.76	5.02	5.95

ture is the scarce amount of information reported on the kinematic performance of the devices. Most of the studies report the error in terms of the percentages of tasks successfully completed compared with the total number of tasks executed. For this type of device focused on the medical field, it is essential to report the final positions of each of the mechanism's phalanges compared to the desired values. Table 5 shows a comparison of the kinematic performance of the exoskeleton reported in this work with those reported by Castiblanco et al. [19] and Gull et al. [74] for the fist and cylindrical

Table 5 – Error comparison of kinematic exoskeleton performance.

Movement	Device	Phalanx	Thumb	Index	Finger Middle	Ring	Little	Error Model
Fist	Reported in [19]	Middle	–	18	17	19	20	Percent
	Our design	Middle	9.42	6.89	7.07	7.20	8.42	Percent
Cylindrical	Reported in [74]	Proximal	3.59	–	8.26	5.9	–	RMSE
		Middle	9.68	–	4.40	3.01	–	RMSE
	Our design	Proximal	2.87	1.90	0.07	0.12	0.07	RMSE
		Middle	3.54	2.76	0.20	0.11	0.15	RMSE

Table 6 – Comparison of different exoskeleton systems for hand rehabilitation.

Reference	EMG signals	Number of fingers	Hand movements	Finger mechanism	Motion capture	Kinematic evaluation	Weight	GUI
Our device	Yes	5	Fist, pinch, cylindrical	Rack-pinion mechanisms	Yes	Yes	730 g	Yes
[19]	Yes	4	Four hand movements	8-bar	No	Yes	Not reported	No
[21]	No	1	Finger flexion	4-bar	No	Yes	Not reported	No
[35]	Yes	5	Cylindrical	4-bar	No	No	950 g	No
[40]	Yes	4	Four hand movements	Pneumatic actuators	No	Yes	Not reported	No
[42]	Yes	5	Three hand movements	Bowden tubes	No	No	258 g	No
[43]	Yes	5	Fingers flexion	Shape memory	No	No	310 g	No
[74]	No	5	Hand open/ close	Soft muscles	No	Yes	Not reported	No
[75]	No	5	Fingers flexion	Bar linkages	Yes	Yes	610 g	No
[76]	No	1	Finger flexion	Bar linkages	No	Yes	45 g	No

grasping movements, respectively. In order to facilitate its interpretation and comparison, the obtained error results reported in Table 4 were also given in terms of the Root Mean Squared Error RMSE.

The exoskeleton reported in [19] only explicitly reports the errors obtained for the middle and distal phalanges of the index, middle, ring and little fingers, while in [74] the results are only reported for the thumb, middle and ring finger for the three phalanges, despite the exoskeleton having been designed for the five fingers of the hand. From Table 5 it can be observed that the design presented in this work has a superior kinematic performance with an error between 6.89% to 9.42% for the middle phalanx in a fist grip compared to other devices that report between 17% to 20% with the error given as a percentage of the mean absolute error (MEA). For a cylindrical grip, the reported RMSE error is in the range of 3.59–8.26 for the proximal phalanx and 3.01–9.68 for the middle phalanx. These values are larger than those reported in this work, with an RMSE error in the range of 0.07–2.87 and 0.11–3.54 for the proximal and middle phalanx, respectively.

One of the advantages of the methodology used in this work is the use of motion capture, which facilitates the trajectory tracking of all the fingers and all the phalanges. This is in contrast to tests which use video analysis techniques where it is only possible to analyze the index finger due to the camera's position. For example, the study by Moreno-SanJuan et al. [75] only reported an error of 6.5% for the index finger of the metacarpal phalanx, while Hsu et al. [76] only reported the results for the finger tip.

Table 6 presents a comparison between the device proposed in this work and other devices previously reported in literature. The characteristics taken into account for this comparison include if the exoskeleton uses EMG signals for its control, the number of fingers that the exoskeleton has, the movements considered for testing, the mechanism used for finger movement, if a motion capture system is used for the kinematic evaluation, the device's weight and the development of a GUI for system operation. As can be observed, neither of the referenced exoskeletons reports a GUI for system operation, while only one [75] uses a motion capture system for evaluating the kinematic performance. Some of the devices have been developed with fewer than 5 fingers [19,21,40,76] or they do not have independent movement for each finger [35].

5. Conclusions

In this article, the design and implementation of an instrumentation and control system for a prototype hand exoskeleton focused on assisted rehabilitation was presented. For

prototyping, the use of 3D printing provides advantages such as obtaining complicated geometries and redesigning in short timeframes for testing. An EMG signal database with three different hand movements was created, which is available in a repository and can be downloaded for free. It can be used by people who work in a similar field of research or for academic purposes, since it is one of the largest databases reported where each of the samples comes from a different person. The kNN algorithm with which the EMG signals were classified obtained the best performance compared to other algorithms, with a result of 81.2%. When the same algorithm was tested with a database of seven tests for one user, results were higher than 95% accurate. Evaluations were made with support vector machines and decision trees, but their performance did not exceed 77% of classification, therefore they were discarded for implementation.

In the performance control evaluation, the maximum error obtained is 10.63% for the proximal phalanx of the index finger in a cylindrical grasp. Physically this difference represents 1.89° less compared to the desired angle. In terms of angular movement, the largest error obtained is 5.7° for the middle phalanx of the index finger for the fist, although its error percentage is equivalent to 6.89%. These obtained results were quantitatively compared with data from similar devices recently reported in the literature showing a superior kinematic performance of the proposed exoskeleton. These results demonstrate that it is possible to use other controller options, such as fuzzy logic, which do not depend on the system model but nevertheless provide accurate performance. Moreover, the developed GUI provides a friendly interaction between the exoskeleton and the user by allowing bidirectional communication between the system and the user. Furthermore, there is even the possibility of extending the database used for the classifier training by adding new test data.

The control and instrumentation for an exoskeleton prototype shown in this article is the first step to a functional system that can later be tested with other users or patients. Therefore, it is susceptible to improvements and changes in the algorithm for signal classification and control. At this stage of the project, the exoskeleton can only be used for symmetrical bilateral movement. Therefore, the asymmetrical bilateral hand movement for interlimb coordination could be considered for another future work.

Declaration of Competing Interest

The authors declare that they have no known competing financial interests or personal relationships that could have appeared to influence the work reported in this paper.

Acknowledgements

The first author thanks CONACyT-Mexico for the support for his graduate studies with the Grant No. 638979. Second and third authors thank CONACyT-Mexico for their support through the Catedras- CONACyT program with project 621.

REFERENCES

[1] Li M, Chen J, He G, Cui L, Chen C, Secco EL, Yao W, Xie J, Xu G, Wurdemann H. Attention enhancement for exoskeleton-assisted hand rehabilitation using fingertip haptic stimulation. Front Robot AI 2021;8:1–13. https://doi.org/10.3389/frobt.2021.602091.

[2] Dindorf R, Wos P. Using the bioelectric signals to control of wearable orthosis of the elbow joint with bi-muscular pneumatic servo-drive. Robotica 2020;38(5):804–18. https://doi.org/10.1017/S0263574719001097.

[3] Tinoco-Varela D, Gudiño-Peñaloza F, Villaseñor-Rodelas CJ. Characterized bioelectric signals by means of neural networks and wavelets to remotely control a human-machine interface. Sensors 2019;19(8):1–21. https://doi.org/10.3390/s19081923.

[4] Al-Quraishi MS, Elamvazuthi I, Daud SA, Parasuraman S, Borboni A. Eeg-based control for upper and lower limb exoskeletons and prostheses: A systematic review. Sensors 2018;18(10):3342. https://doi.org/10.3390/s18103342.

[5] Acharya UR, Fujita H, Oh SL, Hagiwara Y, Tan JH, Adam M, San-Tan R. Deep convolutional neural network for the automated diagnosis of congestive heart failure using ecg signals. Appl Intell 2019;49(1):16–27. https://doi.org/10.1007/s10489-018-1179-1.

[6] Santos-Pessoa de Melo M, Gomes da Silva-Neto J, Natario-Teixeira JMX, Elza-Fontes Da Gama A, Teichrieb V. An emg-based virtual reality application for motor rehabilitation. In: Proceedings of 2019 21st Symposium on Virtual and Augmented Reality (SVR). p. 170–7. https://doi.org/10.1109/SVR.2019.00041.

[7] Armijo PR, Huang CK, High R, Leon M, Siu KC, Oleynikov D. Ergonomics of minimally invasive surgery: an analysis of muscle effort and fatigue in the operating room between laparoscopic and robotic surgery. Surg Endosc 2019;33(7):2323–31. https://doi.org/10.1007/s00464-018-6515-3.

[8] Li M, He B, Liang Z, Zha CG, Chen J, Zhuo Y, Xu G, Xie J, Althoefer K. An attention-controlled hand exoskeleton for the rehabilitation of finger extension and flexion using a rigid-soft combined mechanism. Front Neurorobot 2019;13:1–13. https://doi.org/10.3389/fnbot.2019.00034.

[9] Karabulut D, Ortes F, Arslan YZ, Adli MA. Comparative evaluation of emg signal features for myoelectric controlled human arm prosthetics. Biocybern Biomed Eng 2017;37(2):326–35. https://doi.org/10.1016/j.bbe.2017.03.001.

[10] Sánchez-Velasco LE, Arias-Montiel M, Guzmán-Ramírez E, Lugo-González E. A low-cost emg-controlled anthropomorphic robotic hand for power and precision grasp. Biocybern Biomed Eng 2020;40(1):221–37. https://doi.org/10.1016/j.bbe.2019.10.002.

[11] Wang N, Lao K, Zhang X. Design and myoelectric control of an anthropomorphic prosthetic hand. J Bionic Eng 2017;14(1):47–59. https://doi.org/10.1016/S1672-6529(16)60377-3.

[12] Altin C, Orhan E. Designing wearable joystick and performance comparison of emg classification methods for thumb finger gestures of joystick control. Biomed Res 2017;28(11):4730–6.

[13] Ali S, Samad M, Mehmood F, Ayaz Y, Qazi WM, Khan MJ, Asgher U. Hand gesture based control of nao robot using myo armband. In: Proceedings of Advances in Neuroergonomics and Cognitive Engineering, Springer. p. 449–57. https://doi.org/10.1007/978-3-030-20473-0_44.
[14] Shih-Chieh L, Fong-Gong W, Shu-Hsuanb F. Playing games with your mouth: Improving gaming experience with emg supportive input device. In: Proceedings of International Association of Societies of Design Research Conference.
[15] Carey SL, Lura DJ, Highsmith MJ. Differences in myoelectric and body-powered upper-limb prostheses: Systematic literature review. J Rehabil Res Dev 2015;52(3). https://doi.org/10.1682/JRRD.2014.08.0192.
[16] Jaramillo-Yanez A, Benalcazar ME, Mena-Maldonado E. Real-time hand gesture recognition using surface electromyography and machine learning: A systematic literature review. Sensors 2020;20(9):1–38. https://doi.org/10.3390/s20092467.
[17] Plessis T, Djouani K, Oosthuizen C. A review of active hand exoskeletons for rehabilitation and assistance. Robotics 2021;10(1):1–42. https://doi.org/10.3390/robotics10010040.
[18] Huang Y, Lai WP, Qian Q, Hu X, Tam EWC, Zheng Y. 14 - translation of robot-assisted rehabilitation to clinical service in upper limb rehabilitation. In: Hu X, editor. Intelligent Biomechatronics in Neurorehabilitation. Academic Press; 2020. p. 225–38. https://doi.org/10.1016/B978-0-12-814942-3.00014-3.
[19] Castiblanco JC, Mondragon IF, Alvarado-Rojas C, Colorado JD. Assist-as-needed exoskeleton for hand joint rehabilitation based on muscle effort detection. Sensors 2021;21(13):1–16. https://doi.org/10.3390/s21134372.
[20] Butzer T, Lambercy O, Arata J, Gassert R. Fully wearable actuated soft exoskeleton for grasping assistance in everyday activities. Soft Rob 2021;8(2):128–43. https://doi.org/10.1089/soro.2019.0135.
[21] Akgun G, Cetin AE, Kaplanoglu E. Exoskeleton design and adaptive compliance control for hand rehabilitation. Trans Inst Meas Control 2020;42(3):493–502. https://doi.org/10.1177/0142331219874976.
[22] Kaur A. Machine learning-based novel approach to classify the shoulder motion of upper limb amputees. Biocybern Biomed Eng 2019;39(3):857–67. https://doi.org/10.1016/j.bbe.2019.07.007.
[23] Liu H, Tao J, Lyu P, Tian F. Human-robot cooperative control based on semg for the upper limb exoskeleton robot. Robot Auton Syst 2020;125 . https://doi.org/10.1016/j.robot.2019.103350 103350.
[24] Reyes DA, Daniel Arteaga J, Barrera F. Classifying hand movement intentions using surface emg signals and svm. In: Proceedings of 2019 XXII Symposium on Image, Signal Processing and Artificial Vision (STSIVA). p. 1–5. https://doi.org/10.1109/STSIVA.2019.8730264.
[25] Subasi A. Classification of emg signals using pso optimized svm for diagnosis of neuromuscular disorders. Comput Biol Med 2013;43(5):576–86. https://doi.org/10.1016/j.compbiomed.2013.01.020.
[26] Zhang Z, Yang K, Quian J, Zhang L. Real-time surface emg pattern recognition for hand gestures based on an artificial neural network. Sensors 2019;19(14):1–15. https://doi.org/10.3390/s19143170.
[27] Carlson D, Hsieh Y, Collins E, Carin L, Cevher V. Stochastic spectral descent for discrete graphical models. IEEE J Select Top Signal Process 2016;10(2):296–311. https://doi.org/10.1109/JSTSP.2015.2505684.
[28] Shao J, Niu Y, Xue C, Wu Q, Zhou X, Xie Y, Zhao X. Single-channel semg using wavelet deep belief networks for upper limb motion recognition. Int J Ind Ergon 2020;76 . https://doi.org/10.1016/j.ergon.2019.102905 102905.
[29] Onay F, Mert A. Phasor represented emg feature extraction against varying contraction level of prosthetic control. Biomed Signal Process Control 2020;59 . https://doi.org/10.1016/j.bspc.2020.101881 101881.
[30] Parajuli N, Sreenivasan N, Bifulco P, Cesarelli M, Savino S, Niola V, Esposito D, Hamilton TJ, Naik GR, Gunawardana U, Gargiulo GD. Real-time emg based pattern recognition control for hand prostheses: A review on existing methods, challenges and future implementation. Sensors 2019;19(20):1–30. https://doi.org/10.3390/s19204596.
[31] Benazzouz A, Guilal R, Amirouche F, Hadj Slimane ZE. Emg feature selection for diagnosis of neuromuscular disorders. In: Proceedings of 2019 International Conference on Networking and Advanced Systems (ICNAS). p. 1–5. https://doi.org/10.1109/ICNAS.2019.8807862.
[32] Shi WT, Lyu ZJ, Tang ST, Chia TL, Yang CY. A bionic hand controlled by hand gesture recognition based on surface emg signals: A preliminary study. Biocybern Biomed Eng 2018;38(1):126–35. https://doi.org/10.1016/j.bbe.2017.11.001.
[33] Jiang D, Li G, Sun Y, Kong J, Tao B, Chen D. Grip strength forecast and rehabilitative guidance based on adaptive neural fuzzy inference system using semg. Pers Ubiquit Comput 2019:1–10. https://doi.org/10.1007/s00779-019-01268-3.
[34] Li Z, Guan X, Zou K, Xu C. Estimation of knee movement from surface emg using random forest with principal component analysis. Electronics 2020;9(1):43. https://doi.org/10.3390/electronics9010043.
[35] Leonardis D, Barsotti M, Loconsole C, Solazzi M, Troncossi M, Mazzotti C, Castelli VP, Procopio C, Lamola G, Chisari C, Bergamasco M, Frisoli A. An emg-controlled robotic hand exoskeleton for bilateral rehabilitation. IEEE Trans Haptics 2015;8(2):140–51. https://doi.org/10.1109/TOH.2015.2417570.
[36] Bouteraa Y, Abdallah IB, Elmogy AM. Training of hand rehabilitation using low cost exoskeleton and vision-based game interface. J Intell Robot Syst 2019;96(1):31–47. https://doi.org/10.1007/s10846-018-0966-6.
[37] Arteaga MV, Castiblanco JC, Mondragon IF, Colorado JD, Alvarado-Rojas C. Emg-driven hand model based on the classification of individual finger movements. Biomed Signal Process Control 2020;58 . https://doi.org/10.1016/j.bspc.2019.101834 101834.
[38] Pardoel S, Doumit M. Development and testing of a passive ankle exoskeleton. Biocybern Biomed Eng 2019;39(3):902–13. https://doi.org/10.1016/j.bbe.2019.08.007.
[39] Hazam Majid MS, Khairunizam W, Shahriman A, Zunaidi I, Sahyudi B, Zuradzman M. Emg feature extractions for upper-limb functional movement during rehabilitation. In 2018 International Conference on Intelligent Informatics and Biomedical Sciences (ICIIBMS), vol. 3; 2018. pp. 314–320. doi:10.1109/ICIIBMS.2018.8549932. .
[40] Chen Y, Yag Z, Wen Y. A soft exoskeleton glove for hand bilateral training via surface emg. Sensors 2021;21(2):1–18. https://doi.org/10.3390/s21020578.
[41] Côté-Allard U, Campbell E, Phinyomar A, Laviolette F, Gosselin B, Scheme E. Interpreting deep learning features for myoelectric control: a comparison with handcrafted features. Front Bioeng Biotechnol 2020;8:1–22. https://doi.org/10.3389/fbioe.2020.00158.
[42] Burns MK, Pei D, Vinjamuri R. Myoelectric control of a soft hand exoskeleton using kinematic synergies. IEEE Trans Biomed Circuits Syst 2019;13(6):1351–61. https://doi.org/10.1109/TBCAS.2019.2950145.
[43] Zhang J, Dai J, Chen S, Xu G, Gao X. Design of finger exoskeleton rehabilitation robot using the flexible joint and the myo armband. In Yu H, Liu J, Liu L, Ju Z, Liu Y, Zhou D. (Eds.) Proceedings of Intelligent Robotics and Applications. Springer International Publishing; 2019. pp. 213–225. .

[44] Li YC, Lin KC, Chen CL, Yao G, Chang YJ, Lee YY, Liu CT. Comparative efficacy study of robotic priming of bilateral approach in stroke rehabilitation. Front Neurol 2021;12:1–9. https://doi.org/10.3389/fneur.2021.658567.
[45] Hsu HY, Chiu HY, Kuan TS, Tsai CL, Su LC, Kuo FC. Robotic-assisted therapy with bilateral practice improves task and motor performance in the upper extremities of chronic stroke patients: A randomised controlled trial. Aust Occup Ther J 2019;66(5):637–47. https://doi.org/10.1111/1440-1630.12602.
[46] Chen PM, Kwong PWH, Lai CKY, Ng SSM. Comparison of bilateral and unilateral upper limb training in people with stroke: A systematic review and meta-analysis. PLoS ONE 2019;14(5):1–21. https://doi.org/10.1371/journal.pone.0216357.
[47] Sheng VN, Yanxin Z, Wei M, Chao D, Shengquan X. Bilateral robots for upper-limb stroke rehabilitation: State of the art and future prospects. Med Eng Phys 2016;38(7):587–606. https://doi.org/10.1016/j.medengphy.2016.04.004.
[48] Gandolla M, Niero L, Molteni F, Guanziroli E, Ward NS, Predrocchi A. Brain plasticity mechanisms underlying motor control reorganization: Pilot longitudinal study on post-stroke subjects. Brain Sci 2021;11(3):1–16. https://doi.org/10.3390/brainsci11030329.
[49] Kim H, Miller LM, Fedulow I, Simkins M, Abrams GM, Byl N, Rosen J. Kinematic data analysis for post-stroke patients following bilateral versus unilateral rehabilitation with an upper limb wearable robotic system. IEEE Trans Neural Syst Rehabil Eng 2013;21(2):153–64. https://doi.org/10.1109/TNSRE.2012.2207462.
[50] De la Cruz-Sánchez BA, Arias-Montiel M, Lugo-González E. Development of hand exoskeleton prototype for assisted rehabilitation. In Gasparetto A, Ceccarelli M. (Eds.), Proceedings of Mechanism Design for Robotics. Springer International Publishing: Cham; 2019. pp. 378–385. doi:10.1007/978-3-030-00365-4_45. .
[51] Cotugno G, Althoefer K, Nanayakkara T. The role of the thumb: Study of finger motion in grasping and reachability space in human and robotic hands. IEEE Trans Syst Man Cybern Syst 2017;47(7):1061–70. https://doi.org/10.1109/TSMC.2016.2531679.
[52] Nanayakkara VK, Cotugno G, Vitzilaios N, Venetsanos D, Nanayakkara T, Sahinkaya MN. The role of morphology of the thumb in anthropomorphic grasping: A review. Front Mech Eng 2017;3:5. https://doi.org/10.3389/fmech.2017.00005.
[53] Joseph Vedhagiri GJ, Prituja AV, Li C, Zhu G, Thakor NV, Ren H. Pinch grasp and suction for delicate object manipulations using modular anthropomorphic robotic gripper with soft layer enhancements. Robotics 2019;8(3).
[54] Takata SC, Wade ET, Roll SC. Hand therapy interventions, outcomes, and diagnoses evaluated over the last 10-years: A mapping review linking research to practice. J Hand Ther 2019;32(1):1–9. https://doi.org/10.1016/j.jht.2017.05.018.
[55] Ribeiro TH, Vieira M. Motion capture technology benefits and challenges. Int J Innov Res Technol Sci 2016;48(1). pp. 2321–1156.
[56] De la Cruz-Sanchez BA, Arias-Montiel M, Lugo-González E. Mocap database for three hand movements. Mendeley Data 2020;V2:1. https://doi.org/10.17632/y6r62t56km.1.
[57] Gülke J, Wachter NJ, Geyer T, Schöll H, Apic G, Mentzel M. Motion coordination patterns during cylinder grip analyzed with a sensor glove. J Hand Surg Am 2010;35(5):797–806. https://doi.org/10.1016/j.jhsa.2009.12.031.
[58] Sandoval Gonzalez O, Jacinto Villegas J, Herrera Aguilar I, Portillo Rodiguez O, Tripicchio P, Hernandez Ramos M, Flores Cuautle A, Avizzano C, et al. Design and development of a hand exoskeleton robot for active and passive rehabilitation. Int J Adv Robot Syst 2016;13(66):1–12. https://doi.org/10.5772/62404.
[59] Basteris A, Nijenhuis SM, Stienen AHA, Buurke JH, Prange GB, Amirabdollahian F. Training modalities in robot-mediated upper limb rehabilitation in stroke: a framework for classification based on a systematic review. J Neuroeng Rehabil 2014;11(1):111. https://doi.org/10.1186/1743-0003-11-111.
[60] Yue Z, Zhang X, Wang J. Hand rehabilitation robotics on poststroke motor recovery. Behav Neurol. doi:10.1155/2017/3908135. .
[61] Ding J, Lin R-Z, Lin Z-Y. Service robot system with integration of wearable myo armband for specialized hand gesture human–computer interfaces for people with disabilities with mobility problems. Comput Electr Eng 2018;69:815–27. https://doi.org/10.1016/j.compeleceng.2018.02.041.
[62] De la Cruz-Sanchez BA, Arias-Montiel M, Lugo-González E. semg database of the myo bracelet for hand gestures. Mendeley Data 2019;V1:1. https://doi.org/10.17632/sg9kwnwcp6.1.
[63] Giannakopoulos T, Pikrakis A. Chapter 4 – audio features. In: Giannakopoulos T, Pikrakis A, editors. Introduction to Audio Analysis. Oxford: Academic Press; 2014. p. 59–103. https://doi.org/10.1016/B978-0-08-099388-1.00004-2.
[64] Phukpattaranont P, Thongpanja S, Anam K, Al-Jumaily A, Limsakul C. Evaluation of feature extraction techniques and classifiers for finger movement recognition using surface electromyography signal. Med Biol Eng Comput 2018;56(12):2259–71. https://doi.org/10.1007/s11517-018-1857-5.
[65] Alpaydin E. Introduction to Machine Learning, Adaptive Computation and Machine Learning. MIT Press; 2010.
[66] Padmaja DL, Vishnuvardhan B. Comparative study of feature subset selection methods for dimensionality reduction on scientific data, in. In: Proceedings of 2016 IEEE 6th International Conference on Advanced Computing (IACC). p. 31–4. https://doi.org/10.1109/IACC.2016.16.
[67] Pohjalainen J, Räsänen O, Kadioglu S. Feature selection methods and their combinations in high-dimensional classification of speaker likability, intelligibility and personality traits. Comput Speech Lang 2015;29(1):145–71. https://doi.org/10.1016/j.csl.2013.11.004.
[68] Räsänen O, Pohjalainen J. Random subset feature selection in automatic recognition of developmental disorders, affective states, and level of conflict from speech. In: Proceedings of 14th Annual Conference of the International Speech Communication Association (Interspeech). p. 210–4.
[69] De la Cruz-Sanchez BA, Schoen MP, Perez-Gracia A, Arias-Montiel M, Lugo-González E. Semg pattern recognition for assisted rehabilitation. Proceedings of XXI Congreso Mexicano de Robótica 2019;vol. 1000:186–91.
[70] Farah N, Talib MHN, Mohd Shah NS, Abdullah Q, Ibrahim Z, Lazi JBM, Jidin A. A novel self-tuning fuzzy logic controller based induction motor drive system: An experimental approach. IEEE Access 2019;7:68172–84. https://doi.org/10.1109/ACCESS.2019.2916087.
[71] Acikgoz H. Speed control of dc motor using interval type-2 fuzzy logic controller. Int J Intell Syst Appl Eng 2018;6(3):197–202. https://doi.org/10.18201/ijisae.2018644777.
[72] De la Cruz-Sánchez BA, Arias-Montiel M, Lugo-González E. Trajectory planning and fuzzy control of a hand exoskeleton for assisted rehabilitation. In: Proceedings of Seventh International Workshop on Medical and Service Robots (MESROB2020). Springer International Publishing; 2020. p. 3–11. https://doi.org/10.1007/978-3-030-58104-6_1.
[73] Iancu I. A mamdani type fuzzy logic controller. In: Dadios EP. (Ed.), Fuzzy Logic. IntechOpen: Rijeka; 2012, Ch. 16. pp. 325–350. doi:10.5772/36321. .

[74] Gull MA, Bai S, Blicher JU, Stærmose TG. Design and performance evaluation of a hybrid hand exoskeleton for hand opening/closing. J Med Devices 2021;15(4):1–10. https://doi.org/10.1115/1.4052448.
[75] Moreno-San Juan V, Cisnal A, Fraile JC, Pérez-Turiel J, De-la Fuente E. Design and characterization of a lightweight underactuated raca hand exoskeleton for neurorehabilitation. Rob Auton Syst 2021;143 . https://doi.org/10.1016/j.robot.2021.103828 103828.
[76] Hsu TH, Chiang YC, Chan WT, Chen SJ. A finger exoskeleton robot for finger movement rehabilitation. Inventions 2017;2 (3):1–8. https://doi.org/10.3390/inventions2030012.